

Solid state ^{29}Si and ^{31}P NMR study of gel derived phosphosilicate glasses

Nigel J. Clayden,^a Serena Esposito,^b Pasquale Pernice*^b and Antonio Aronne^b

^aSchool of Chemical Science, University of East Anglia, Norwich, UK NR4 7TJ

^bDepartment of Materials and Production Engineering, University of Naples Federico II, Piazzale Tecchio, 80125 Napoli, Italy. E-mail: pernice@unina.it

Received 23rd May 2000, Accepted 21st November 2000

First published as an Advance Article on the web 24th January 2001

Solid state ^{29}Si and ^{31}P MAS NMR have been used to investigate the microstructural changes occurring in phosphosilicate gels during their conversion from a gel to the corresponding gel-derived glasses by heating. The studied gels have the molar compositions $10\text{P}_2\text{O}_5\cdot 90\text{SiO}_2$ and $30\text{P}_2\text{O}_5\cdot 70\text{SiO}_2$. It was found that the dried gels (100°C) have very similar structures formed by a siloxane framework containing silanol groups and including trapped molecules of orthophosphoric acid along with a very small amount of pyrophosphoric acid. In spite of this initial similarity further heating causes markedly different structural rearrangements of their glassy matrices. Namely, the co-polymerisation of phosphate and silicate tetrahedra takes place at 300°C for the gel with the higher phosphorus content whereas this occurs only after heat treatment for 30 minutes at 400°C for the gel with the lower phosphorus content. Moreover, the presence of six-coordinated silicon in the glassy matrix of the $30\text{P}_2\text{O}_5\cdot 70\text{SiO}_2$ gel has been observed. The different evolution of the investigated gel microstructures mirrors their different crystallization behaviour: $10\text{P}_2\text{O}_5\cdot 90\text{SiO}_2$ keeps its amorphous nature up to 1000°C while for $30\text{P}_2\text{O}_5\cdot 70\text{SiO}_2$ crystallization starts after heat treatment for 30 minutes at 400°C .

1. Introduction

Phosphosilicate glasses exhibit interesting technological and structural properties. They find applications as fast proton conductors^{1–3} and as bioactive elements when present in certain chemical compositions.⁴ A particular feature of the alkali^{5–7} and alkaline-earth⁸ phosphosilicate glasses is that a fraction of the Si^{4+} ions are octahedrally coordinated as also seen in certain crystalline phosphosilicates including $\text{Si}_5\text{O}(\text{PO}_4)_6$,⁹ $\text{Si}_3(\text{PO}_4)_4$,¹⁰ and SiP_2O_7 .¹¹ It is also worth noting that crystalline silicon diphosphate exists in various polymorphs in which all the silicon atoms are six-coordinated.¹¹ Although these materials can be prepared by the conventional ceramic route, sol–gel synthetic methods are a viable alternative not only because they represent a lower cost technology but also because better mixing of the starting materials at the molecular level can be achieved. This allows the preparation of a high purity ceramic in its final film shape, by dipping or spin-coating, with a homogeneous distribution of components on the atomic scale.^{12,13} However, viewed from the perspective of achieving a homogeneous composition, the chemistry of the sol–gel synthesis of phosphosilicate glasses appears to be anomalous.^{14–19} On the one hand, Livage *et al.*¹⁴ have shown that phosphate esters, $\text{PO}(\text{OR})_3$, react too slowly with water under ambient conditions to be easily used as the molecular precursors of P_2O_5 in the sol–gel synthesis of silicophosphate materials. On the other hand orthophosphoric acid, $\text{PO}(\text{OH})_3$, reacts too fast in comparison with tetraethoxysilane (TEOS) and it can lead to precipitation rather than gelation. More convenient precursors can be obtained either by dissolving P_2O_5 in alcohols forming different $\text{PO}(\text{OH})_{3-x}(\text{OR})_x$ species that exhibit chemical reactivity intermediate between $\text{PO}(\text{OR})_3$ and $\text{PO}(\text{OH})_3$, or by using phosphoryl chloride, POCl_3 . Tian *et al.* by NMR¹⁵ and Szu *et al.* by MAS NMR¹⁶ found no evidence for the formation of either P–O–Si or P–O–P linkages in the sol or in the dried gels but only in the heat treated gels using $\text{PO}(\text{OC}_2\text{H}_5)_3$,^{15,16} $\text{PO}(\text{OH})_3$ and $\text{P}(\text{OCH}_3)_3$.¹⁶ Yet, the type of precursor strongly affects the structure of the gel

derived glasses and their crystallization behavior.¹⁶ In addition, the amount of phosphorus lost during the heat treatment used to convert the gel into the final product was dependent on the type of phosphorus molecular precursor¹⁶ as well as the preparation method.¹⁷ Laczka and Ciecinska¹⁸ observed that the nature of the phosphorus molecular precursors ($\text{PO}(\text{OC}_2\text{H}_5)_3$, $\text{PO}(\text{OH})_3$ and POCl_3) affects the crystallization behaviour of the gel glasses but it has no influence on their structures. Kim and Tressler¹⁹ have examined the thermal evolution of phosphosilicate gel containing 56 mol% P_2O_5 using $\text{PO}(\text{OH})_3$ as the phosphorus molecular precursor. They found that $\text{Si}_3(\text{PO}_4)_4$ was the main phase in low temperature ($\sim 300^\circ\text{C}$) heat treated samples, while for higher temperatures ($\sim 800^\circ\text{C}$) SiP_2O_7 becomes the main crystallizing phase.¹⁹ Recently, Cao *et al.*²⁰ have synthesized phosphosilicate gels with a P_2O_5 content ranging from 10 to 50 mol% using P_2O_5 as the phosphorus molecular precursor. By ^{29}Si and ^{31}P MAS NMR they observed hexacoordinated silicon in the dried (at 100°C) gel samples. Moreover, it was observed that in the gel samples fired at 700°C the crystallization of $\text{Si}_5\text{O}(\text{PO}_4)_6$ occurs independently of the starting gel composition and that this process starts at 300°C .²⁰

It has long been appreciated that a full understanding of both the structure and the relationship between the basic structure and glass properties is a fundamental prerequisite in the design of materials. Such an understanding requires knowledge not only of the types of structural units present and their relative concentrations but also of the transformations they undergo as a result of the heat treatments employed.

In a recent paper³ we reported the sol–gel synthesis of humidity-sensitive phosphosilicate thin films and bulk gels having the molar composition $10\text{P}_2\text{O}_5\cdot 90\text{SiO}_2$ and $30\text{P}_2\text{O}_5\cdot 70\text{SiO}_2$ using POCl_3 as the phosphorus molecular precursor. The FTIR spectra clearly showed that, for both compositions, the transformations in the corresponding gel-derived glasses were complete at 1000°C . Additionally, at this temperature, crystallization of the $\text{Si}_3(\text{PO}_4)_4$ phase starts for the gel derived glass with the higher phosphorus content. It was

also found that the phosphorus content and the temperature of the heat treatment strongly affect the sensitivity of the gel-derived films to the relative humidity. In this paper we report a detailed ^{29}Si and ^{31}P MAS NMR investigation of the structure of the above phosphosilicate bulk gels as a function of the heat treatment.

2. Experimental

Phosphoryl chloride, POCl_3 (99%, Aldrich), and tetraethoxysilane, $\text{Si}(\text{OC}_2\text{H}_5)_4$ (99%, Gelest; TEOS), were used as starting materials in the sol-gel preparation. Two compositions of phosphosilicate sols were prepared: $10\text{P}_2\text{O}_5 \cdot 90\text{SiO}_2$ (10P) gel and $30\text{P}_2\text{O}_5 \cdot 70\text{SiO}_2$ (30P) gel using a procedure that has been reported in a previous paper.³ Complete gelation occurred at room temperature in 10 days for the 10P gel and in 14 days for the 30P gel. The gelled systems were held for one more day at room temperature before drying. The gels were fully dried in air at 100°C in an electric oven for one day. After these treatments transparent and amorphous bulk gels were obtained for both compositions.

Quantitative analysis of the phosphorus and silicon contents in the gel-derived glasses was performed for both gels. The two oxides were separated according to the procedure reported in ref. 21. The SiO_2 content was then determined by the gravimetric method. The phosphorus content was determined colorimetrically by conversion to the blue phosphomolybdate complex formed by phosphorus and molybdenum in the presence of a suitable reducing agent.²²

The nature and temperatures of the various reactions occurring during the heating of the dried gels were determined by differential thermal analysis (DTA) using a Netzsch thermoanalyser High Temperature DSC 404 with Al_2O_3 as the reference material. The DTA curves, recorded at a heating rate of 10 K min^{-1} , were recorded for bulk samples, 30 mg, of the dried gels. Temperatures detected on DTA curves are accurate to $\pm 1\text{ K}$.

The amorphous nature of the dried gels as well as the nature of the crystallizing phases were ascertained by X-ray diffraction using a Philips diffractometer model PW1710 ($\text{CuK}\alpha$) with a scan speed of 1° min^{-1} .

Solid state ^{31}P NMR spectra were acquired on a Bruker MSL-200 NMR spectrometer operating at 81.0 MHz. Magic angle sample spinning (MAS) was carried out using a Bruker double bearing rotor system with 7 mm zirconia rotors. Typical spinning speeds were 4 kHz, which was sufficient to make the spinning sidebands of low intensity and outside the region of interest. A 90° pulse of $5\ \mu\text{s}$ together with a recycle delay of 150 s was used over a spectral width of 40 kHz. 40 transients were collected. ^{29}Si NMR data were collected on a JEOL GX-400 equipped with a solid state NMR accessory, operating at 79.5 MHz. The probe is of a double bearing design using 4 mm zirconia rotors. A 45° pulse of $3\ \mu\text{s}$ duration was used together with a recycle delay of 180 s over a spectral width of 40 kHz. The choice of recycle delay was based on previous literature values together with the results obtained in control experiments with recycle delays of 60 s, 180 s and 300 s. No relative saturation effects were seen when the recycle delay was decreased from 300 s to 180 s. Typically a spinning speed of

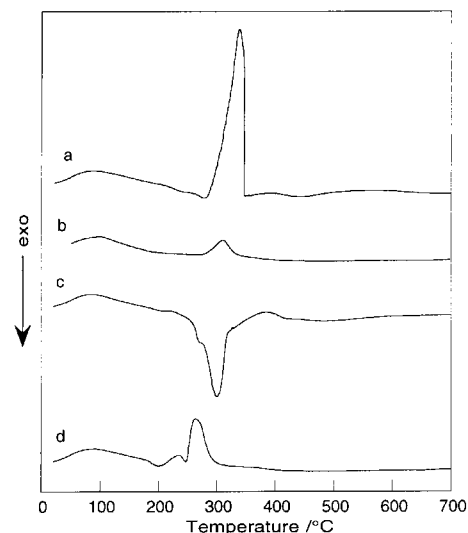


Fig. 1 DTA curves of the dried gels recorded at 10 K min^{-1} : (a) 10P in air; (b) 10P in argon; (c) 30P in air; (d) 30P in argon.

6 kHz was used and 300 transients were acquired. All spectra were acquired with fully loaded rotors. The ^{31}P chemical shifts were referenced using the secondary reference γ -zirconium phosphate taking the more shielded resonance as -9.7 ppm with respect to 85% phosphoric acid. The siloxane Q_8M_8 was used as a ^{29}Si secondary reference taking the M type resonance as $+11.5\text{ ppm}$.

3. Results

Table 1 lists results of the chemical analysis of the studied gel derived glasses. For both gels the analysed compositions are in very good agreement with the nominal composition showing that the applied synthesis procedure³ strongly reduces the phosphorus loss in the gel-derived glasses. Therefore, the samples henceforth are labelled by their nominal compositions of P_2O_5 .

Fig. 1 shows the DTA curves of the dried gels recorded in air and in argon. A broad endothermic peak, from room temperature to about 200°C , appears on all the DTA curves because of the evaporation of water and alcohol physically trapped in the gels through open pores in the gel. The DTA curves of the 10P dried gel in air, Fig. 1(a), and in argon, Fig. 1(b), exhibit an endothermic peak at about 300°C that is enhanced in air. In the same temperature range the DTA curve recorded in air of the 30P dried gel, Fig. 1(c), shows two unresolved exothermic peaks that appear as well resolved endothermic peaks on the DTA curve of the same sample recorded in argon, Fig. 1(d).

The XRD patterns of the dried gels as well as those of the heat treated gel samples are shown in Fig. 2. The 10P gel keeps its amorphous nature up to 1000°C , Fig. 2(e) and (f), whereas the XRD pattern of the 30P gel sample heat treated for 30 min at 400°C , Fig. 2(b), exhibits a few broad reflections arising from the amorphous background indicating the precipitation of very small crystallites in the amorphous matrix. As these crystals are not well formed their precise identification is hindered. Thus the observed d -spacing values match three different phosphosilicate phases: $3\text{SiO}_2 \cdot 2\text{P}_2\text{O}_5$ (JCPDS card 22-1380), $5\text{SiO}_2 \cdot 3\text{P}_2\text{O}_5$ (JCPDS card 40-457) and $\text{Si}(\text{HPO}_4)_2 \cdot \text{H}_2\text{O}$ (JCPDS card 18-1168). The first two contain silicon in four-fold and six-fold coordination and their crystal structures differ only in the relative amounts of SiO_6 groups with respect to SiO_4 groups.^{9,10} On the other hand only SiO_6 groups are present in the structure of the $\text{Si}(\text{HPO}_4)_2 \cdot \text{H}_2\text{O}$ phase, the anhydrous analogue of which is crystalline SiP_2O_7 .¹⁸ The next heat treatment (1000°C) causes the growth of the

Table 1 Chemical analysis for gel-derived glasses heated at 1000°C

Sample	Nominal composition (mol%)		Analyzed composition ^a (mol%)	
	P_2O_5	SiO_2	P_2O_5	SiO_2
10P	10	90	10.2	89.7
30P	30	70	27.9	71.3

^aThe errors are within 2%.

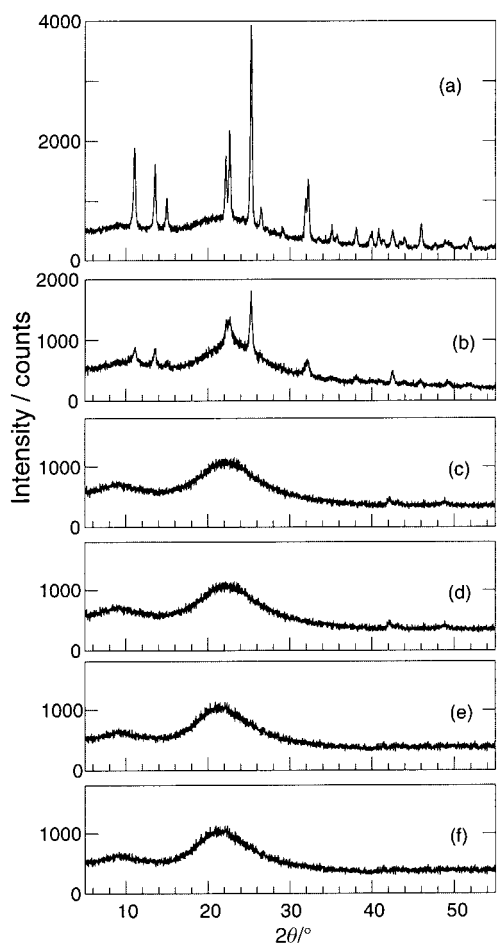


Fig. 2 XRD patterns of the gel samples heated at 2 K min⁻¹: (a) 30P 1000 °C; (b) 30P 400 °C for 30 min; (c) 30P 300 °C; (e) 10P 1000 °C; and of the dried gels: (d) 30P; (f) 10P.

crystallites previously formed, giving rise to sharp reflections on the amorphous background, Fig. 2(a). This XRD pattern gave a good match with JCPDS cards 22-1380 and 40-457.

For the ³¹P and ²⁹Si NMR study of the thermal transformation of the phosphosilicate gel, gels heated to three temperatures: 300 °C, 400 °C and 1000 °C, as well as the dried gel itself were used. These temperatures were chosen on the basis of the thermal analysis data. In each case the sample was prepared by slow heating at 2 K min⁻¹ to the required temperature and then quenching. Additionally the 400 °C sample was held at this temperature for 30 min. Observed chemical shifts of the ²⁹Si and ³¹P resonances of the studied gels are listed in Table 2. Curve fitting of the ²⁹Si NMR spectra was

Table 2 Chemical shifts, δ , of the ²⁹Si and ³¹P resonances observed for the studied gels. ³¹P and ²⁹Si chemical shifts are accurate to within 0.11 and 0.12 ppm respectively based on the digital resolution of the NMR spectra

	100 °C		300 °C		400 °C		1000 °C	
	δ ²⁹ Si	δ ³¹ P	δ ²⁹ Si	δ ³¹ P	δ ²⁹ Si	δ ³¹ P	δ ²⁹ Si	δ ³¹ P
10P	-100	-1.4	—	0	—	0	—	—
	-109	-12	-111	-12	-114	-12	-118	—
				-23		-23		—
								-37
30P	-100	-1.4	—	0	—	0	—	—
	-109	-12	—	-10	—	-10	—	—
			-115	-24	-115	-24	-115	—
			—	-30	—	-30	-120	-35
			-211	-42	-211	-42	-215	-44
		-215	-44	-215	-44	-215	-44	
						-218		

also performed using gaussian functions and the results are listed in Table 3. In the curve fitting the minimum number of gaussian functions was chosen to represent the NMR spectrum rather than a number based on a preconceived idea of a particular coordination giving rise to a resonance at a defined chemical shift. Since the broad resonances observed in the ²⁹Si NMR spectra prevent the resolution of individual resonances corresponding to all the different types of silicon coordination, in any comparison of the integrated intensities it must be borne in mind that the gaussian function may represent different silicon environments, for example Si(OSi)₄ and Si(OSi)₃(OP)/(OH). In general errors associated with the standard errors of the gaussian parameters found in the fitting procedure were small, less than 2%. This, however, will understate the true error in the intensity associated with a particular environment since it is not possible to apportion intensity arising from different environments in an overlapping resonance.

Cross-linking in the ²⁹Si and ³¹P NMR spectra can be denoted by the Q_N and Q'_N notation where Q_N indicates Si(OSi)_N(OX)_{4-N} and Q'_N stands for OP(OP)_N(OX)_{3-N}. For the 10P gel the ²⁹Si MAS NMR spectrum of the dried sample exhibits two resonances at -100 and -109 ppm, Fig. 3, assigned to silicon tetrahedra connected either to three other silicon tetrahedra and one OH terminal group, Q₃, or to four other silicon tetrahedra, Q₄.^{16,23,24} The resonance at -109 ppm is slightly shifted to lower chemical shift (-111 ppm) in the ²⁹Si MAS NMR spectrum of 10P-300 and shows a shoulder at -100 ppm, Fig. 3. For 10P-400 and 1000 a single resonance at -114 ppm appears in their ²⁹Si MAS NMR spectra, the linewidth of the resonances increasing with the treatment temperature, Fig. 3. The ³¹P MAS NMR spectrum of the dried

Table 3 Chemical shifts, δ , estimated relative intensities, I , and full width at half maximum, Fw (ppm), calculated from line fitting of the ²⁹Si resonances. Standard errors for the relative intensities are less than 0.02 based on the standard errors determined for the gaussian heights and widths

	100 °C			300 °C			400 °C			1000 °C		
	δ	I	Fw	δ	I	Fw	δ	I	Fw	δ	I	Fw
10P	-96.8	0.15	15.8	—	—	—	—	—	—	—	—	—
	-102.3	0.39	5.7	-103.3	0.29	8.6	-103.6	0.17	8.1	-100.0	0.11	8.2
	-110.6	0.46	7.8	-111.9	0.71	9.2	-114.0	0.83	10.2	-114.0	0.89	12.3
30P	-102.5	0.41	5.6	-104.5	0.08	7.0	-103.5	0.08	7.3	—	—	—
	-110.8	0.59	8.3	-115.2	0.84	10.6	-114.9	0.82	12.0	-115.0	0.74	13.3
										-119.6	0.09	2.7
				-210.9	0.04	2.6	-210.9	0.04	4.1	-213.7	0.13	3.0
				-214.4	0.04	4.5	-214.9	0.06	5.1	-217.3	0.04	2.2

Resonance assignments: -95.0 to -100.0 ppm, Q₂: Si(OSi)₂(OH)₂; -100.0 to -103.0 ppm, Q₃: Si(OSi)₃(OH), Q₂: Si(OSi)(OH)₂(OP); -110.0 to -112.0 ppm, Q₄: Si(OSi)₄, Q₃: Si(OSi)₂(OP)(OH); -114.0 to -120.0 ppm, Q₄: Si(OSi)_{4-x}(OP)_x, x = 1 to 3; -210.0 to -220.0 ppm, [SiO₆] six-coordinated silicon.

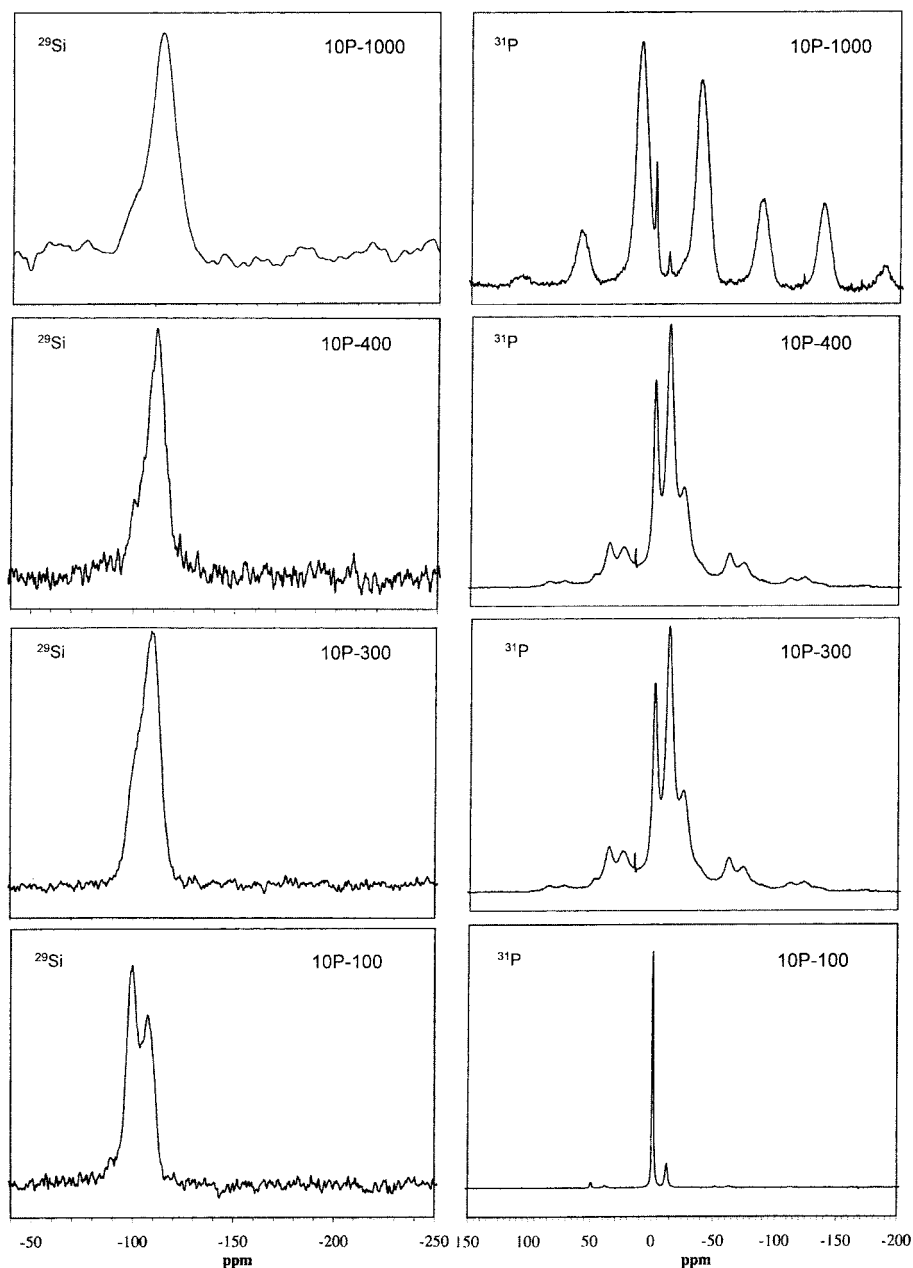


Fig. 3 ^{29}Si and ^{31}P MAS NMR spectra of the gels containing 10% P_2O_5 (10P) at different stages of heat treatment. For ^{31}P MAS NMR spectra the resonances lying outside -5 to -50 ppm are spinning sidebands.

10P gel shows an intense and narrow resonance at -1.4 ppm, Q'_0 , and a smaller one at -12 ppm, Q'_1 , Fig. 3. These resonances can be assigned to orthophosphate and pyrophosphate species, respectively.^{25,26} Despite the solid appearance of this sample the narrow line and low intensity spinning sidebands of the resonance at -1.4 ppm are indicative of a high degree of mobility for the chemical species giving rise to this resonance. After heat treatment at a higher temperature, 10P-300, the ^{31}P resonance at -12 ppm is greatly enhanced with respect to that at *ca.* 0 ppm in the spectrum and, simultaneously, a new resonance at -23 ppm, related to Q'_2 or metaphosphate groups,^{25,26} appears, Fig. 3. The presence of sidebands in the spectra indicates that the cross-linked phosphorus is held rigidly. In addition the broadening of the Q'_0 resonance shows that qualitatively this group is now being held more rigidly, though it is difficult to be more precise in the absence of detailed NMR relaxation time data. Heating the 10P gel to 400°C causes further profound changes in the ^{31}P MAS NMR spectrum. To some extent the changes are misleading, because of the loss in intensity of the Q'_1 resonance and its

replacement by a broad resonance around -30 ppm assigned to Q'_3 .^{25,26} Although the Q'_0 resonance is intense, the integrated intensity is relatively low, because it is narrow, and is in fact unchanged with respect to the overall integrated intensity associated with the rest of the spectrum. Finally, after heating to 1000°C the ^{31}P MAS NMR spectrum is dominated by a single isotropic resonance at -37 ppm flanked by a series of intense sidebands. This pattern is consistent with a phosphoryl group $\text{O}=\text{P}(\text{OP}/\text{Si})_3$ indicating the presence in the glassy network of $[\text{PO}_4]$ tetrahedra linked with either phosphorus or silicon atoms.^{5,8} It is not possible to differentiate between cross-linking between phosphorus and silicon based simply on the ^{31}P chemical shift. Turning to the 30P composition, no differences were seen in the chemical shifts of the ^{31}P and ^{29}Si MAS NMR spectra of the dried gel compared with the corresponding sample of the 10P gel, Fig. 4, although differences were seen in the relative proportions of the Q_N units. In marked contrast, the spectra of the 30P heat-treated samples are significantly different from those of the 10P gel heat-treated samples. This is apparent even at the lowest

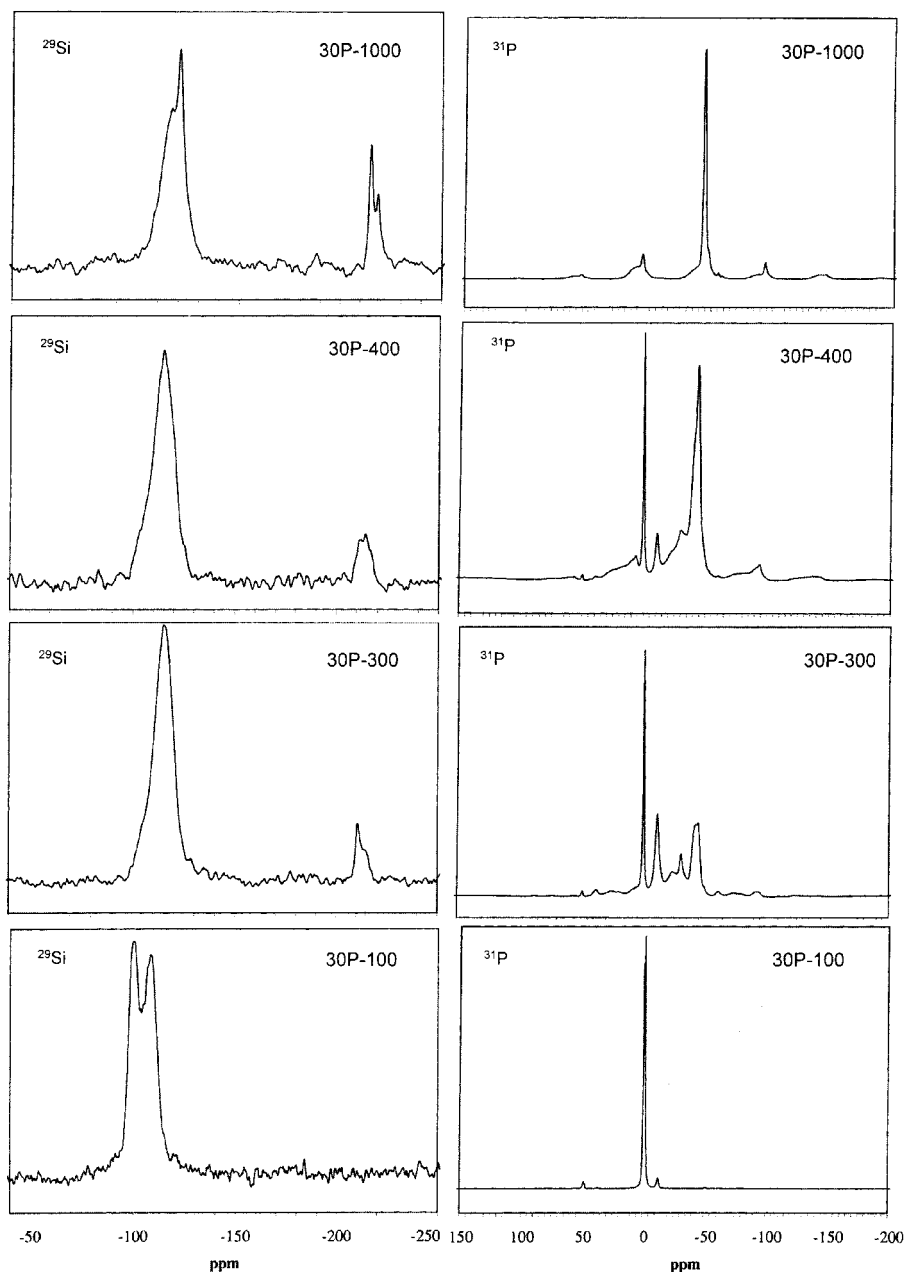


Fig. 4 ^{29}Si and ^{31}P MAS NMR spectra of the gels containing 30% P_2O_5 (30P) at different stages of heat treatment. For ^{31}P MAS NMR spectra the resonances lying outside -5 to -50 ppm are spinning sidebands.

temperature used, 300°C . Thus, the ^{29}Si MAS NMR spectrum of 30P-300 has resonances with chemical shifts typical of six-coordinated silicon, -211 and -215 ppm,^{7,23,24} as well as an intense resonance at -115 ppm, Fig. 4. While in the ^{31}P MAS NMR spectrum of 30P-300, besides the narrow resonance at 0 ppm associated with Q'_0 , additional resonances appear at -10 , -24 , and -30 , assigned to Q'_1 , Q'_2 and Q'_3 respectively. Moreover, two resonances are also seen at -42 and -44 ppm, Fig. 4. These last two resonances are assigned to $[\text{PO}_4]$ tetrahedra linked to $[\text{SiO}_6]$ octahedra and $[\text{SiO}_4]$ tetrahedra.²⁷ For the 30P gel heating at higher temperatures did not substantially alter the ^{29}Si MAS NMR spectra whereas notable changes were observed in the ^{31}P MAS NMR spectra, Fig. 4. In particular, increasing temperature in the heat treatments led to an increase in the relative intensity of the resonance at -44 ppm and a decrease in the intensity of all the other resonances. Indeed, after heating to 1000°C , 30P-1000, the ^{31}P MAS NMR spectrum only shows significant intensity in two resonances, one a narrow resonance at -44 ppm with relatively low intensity spinning sidebands consistent with a rather

symmetric PO_4 environment. The other is a broad peak at *ca.* -35 ppm with a series of associated spinning sidebands arising from a phosphoryl group $\text{O}=\text{P}(\text{OP}/\text{Si})_3$.

4. Discussion

The different behaviour of the two studied gels on heating, Fig. 1, clearly demonstrates that the pyrolysis of residual organic groups in the gels is dependent on the phosphorus content of the gel (residual organic groups being those which have not reacted at the end of the drying step and are not subsequently lost from the gels by evaporation before calcining). In the 30P dried gel the pyrolysis products burn in air, Fig. 1(c), while in the case of the 10P dried gel they evaporate without burning, Fig. 1(a). This result can be related to the differing nature and amount of the intermediate compounds originating in the dehydration process of the gel samples studied. Confirmation of this is provided by the absorption bands in the $2000\text{--}3000\text{ cm}^{-1}$ region in the FTIR.³ Thus in the FTIR spectrum of the 10P dried gel a low intensity

absorption band at 2990 cm^{-1} was seen that was strongly enhanced in the FTIR spectrum of the 30P dried gel. This band was related to the stretching mode of the C–H bond in an aldehydic group.³ The different amounts of these molecules, produced by partial oxidation of ethanol during the dehydration process of the gel samples, can explain the different DTA curves shown in Fig. 1. In both cases the loss of carbon residues was complete by $400\text{ }^{\circ}\text{C}$, Fig. 1.

Silicate glass structure is usually described in terms of Q_N basic structural units ($[\text{SiO}_4]$ tetrahedra) with N bridging oxygen atoms, N ranging between 0 and 4.^{23,24} By analogy, the phosphate glass structure is described by Q'_N basic structural units ($[\text{PO}_4]$ tetrahedra) with N bridging oxygen atoms, N ranging between 0 and 3.^{25,26} Comparison of the ^{29}Si and ^{31}P MAS NMR spectra of both dried gels (10P- and 30P-100), Fig. 3 and 4, indicates that their structures contain the same kind of structural unit consisting of a siloxane matrix with trapped phosphorus precursor monomer. Previous studies of phosphosilicate gels by ^{29}Si NMR have shown that the chemical shift moves to more negative values as the silicon is replaced by phosphorus, and moves to less negative values as the silicon is replaced by hydroxyl groups.^{7,23,24} As the observed chemical shift of quartz is -107 ppm ²³ we can assign the ^{29}Si resonances, -109 and -100 ppm , to a Q_4 unit and a Q_3 unit where one silicon is replaced by a hydroxyl group, $\text{Si}(\text{OSi})_3(\text{OH})$, respectively. Thus the ^{29}Si NMR again provides no evidence for Si–O–P formation in a dried gel. Similarly the isotropic chemical shifts of ^{31}P become more negative with increasing values for N in Q'_N units.^{25,26} So the ^{31}P resonances, -1.4 and -12 ppm , Fig. 3 and 4, can be related to Q'_0 (orthophosphate) and Q'_1 (pyrophosphate) units, respectively, confirming the absence of Si–O–P links at this stage. In addition, as noted earlier, the narrow linewidth of the Q'_0 resonances suggests that this species is mobile and hence not bonded to the rest of the network, merely trapped within the matrix. Given the lack of modifier cations in the gel compositions to balance the charge of nonbridging oxygens together with the FTIR evidence, stretching vibration modes of O–H bonds,³ the Q_N and Q'_N units with nonbridging oxygens are bonded to hydrogen atoms. On the basis of this discussion and consistent with references 15 and 16 we can exclude the formation of Si–O–P bonds in the structures of both dried gels. Hence the dried gels have a three-dimensional siloxane framework containing silanol groups together with isolated molecules of orthophosphoric acid and a very small amount of pyrophosphoric acid. Quite large differences are seen in the relative proportions of the Q_N units in the dried gels, Table 3, indicating a greater degree of cross-linking in the siloxane framework of the 30P gel. However, the relevance of this to the subsequent evolution of the gel on heating is unclear, particularly given that both the 10P and 30P gels show less extensive cross-linking than previously reported dried gels¹⁶ and yet mirror the changes seen in these gels. In spite of the general similarity in the nature of the dried gels, heating them to $300\text{ }^{\circ}\text{C}$ results in a very different evolution of the gel structures even if in both gels no crystallization occurs as shown in Fig. 2. For the 10P gel the appearance of a new ^{31}P resonance at -23 ppm (Q'_2) with the simultaneous increase in the relative intensities of the resonance at -12 ppm with respect to the one at 0 ppm indicates the formation of a more polymerised phosphorus species, Fig. 3. These species are trapped in the siloxane framework but still do not appear to be cross-linked with it. Thus, if phosphorus were present in the siloxane network a significant shielding of the ^{29}Si resonance resulting in a more negative chemical shift would be expected whereas the observed chemical shift for 10P-300 is only slightly more negative (2 ppm) than that of 10P-100, Fig. 3. Furthermore, there was no evidence for a new resonance around -115 ppm . Curve fitting of the ^{29}Si NMR spectrum confirms that two resonances at -103.3 and -111.9 ppm alone are

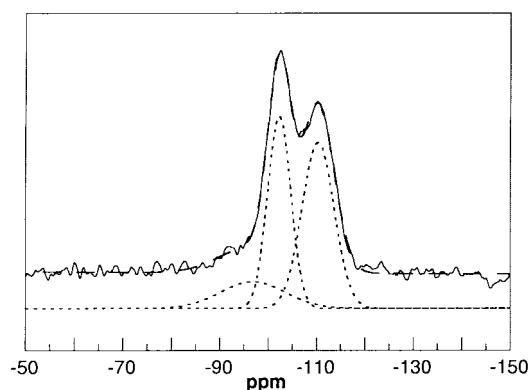


Fig. 5 Comparison of the experimental ^{29}Si NMR spectrum for 10P-100 and the calculated one obtained by curve fitting using gaussian functions. The solid line denotes the experimental data, the dotted lines the individual resonances and the dashed line the sum of the individual calculated resonances.

sufficient to explain the observed lineshape, Table 3. A representative curve fit to the ^{29}Si NMR spectrum of the 10P-100 sample is shown in Fig. 5 to illustrate the good agreement between the experimental and calculated spectra. While there is no evidence for asymmetry on the more shielded side as one might expect if a new resonance around -115 ppm arising from Si–O–P groups were present, it is not possible to rule out completely the formation of Si–O–P bonds since the resonance does become more shielded and more importantly becomes broader. This result, together with the decrease in the relative intensity of the resonance at -100 ppm which appears as a shoulder in the ^{29}Si MAS NMR spectrum of 10P-300, suggests that the heat treatment at $300\text{ }^{\circ}\text{C}$ favours self-dehydroxylation reactions. In other words the silanol groups react with themselves preferentially to increase the degree of cross-linking of the siloxane network while self-condensation between P–OH groups forms more pyrophosphoric acid and also metaphosphoric acid rather than cross-dehydroxylation between P–OH and Si–OH. In marked contrast cross-condensation leading to the formation of Si–O–P bonds was observed when the 30P gel was heated to $300\text{ }^{\circ}\text{C}$. Evidence for the formation of Si–O–P bonds is provided by the ^{29}Si resonances at -211 and -215 ppm which are characteristic of six-coordinated silicon in phosphosilicates known to contain such bonds by X-ray crystal diffraction.^{7–9} Also the Q_4 resonance at -115 ppm is more shielded than expected for $\text{Si}(\text{OSi})_4$ coordination, a change in chemical shift consistent with the presence of one or more phosphorus atoms in the second coordination sphere.^{7–9} Cross-condensation is further confirmed by the appearance in the corresponding ^{31}P MAS NMR spectrum of the resonances at -30 , -42 and -44 ppm , Fig. 4. The chemical shifts seen for the last two resonances are very close to the observed value for the isotropic chemical shift (-44 ppm) of the $\text{Si}_5\text{O}(\text{PO}_4)_6$ phase,²⁸ the structure of which contains $[\text{PO}_4]$ tetrahedra linked to $[\text{SiO}_6]$ octahedra and $[\text{SiO}_4]$ tetrahedra,⁹ while the resonance at -30 ppm corresponds to Q'_3 species with P–O–Si bonds, such as $\text{Si}(\text{HPO}_4)_2\cdot\text{H}_2\text{O}$.^{18,28} Interestingly, the ^{31}P MAS NMR spectrum of 30P-300 still shows the narrow resonance at 0 ppm together with those at -10 and -24 ppm , Fig. 4. In this case the resonance at -24 ppm may be related to metaphosphate chains with P–O–Si terminal units⁷ while the resonance at 0 ppm suggests that some of the phosphorus atoms are still not cross-linked with the siloxane network but remain as molecules of ortho- and pyrophosphoric acid trapped in the phosphosilicate network. The resonances characteristic of six-coordinate silicon demonstrate clearly that the reactions taking place cannot be considered simply as one between Si–OH and P–OH leading to Si–O–P bonds. More complex structural re-organisation

must occur at the same time. In this context it is worthwhile noting that this is the first observation of the presence of both six-coordinate silicon and $[\text{SiO}_4]$ tetrahedra linking $[\text{PO}_4]$ tetrahedra in the glassy matrix of a silicophosphate gel-derived glass.

The ^{29}Si MAS NMR spectrum of the 10P gel after heating at 400°C for 30 min shows a single resonance at -114 ppm, Fig. 3. This resonance appears to be broader on the more shielded side in comparison with the one present in the spectrum of the 10P-300 sample. Confirmation of this resonance is provided by the curve fitting shown in Table 3 which gave two resonances at -103.6 and -114.0 ppm. The change in the chemical shift of the Q_4 type resonance together with the decrease in the intensity of the Q_3 resonance indicates that cross-linking between silicon and phosphorus begins to appear in the amorphous matrix of the 10P gel after this heat treatment. Broadening of the more shielded ^{29}Si resonance for which the full width at half maximum increases from 9.2 ppm to 10.2 ppm, Table 3, is consistent with the formation of Si-O-P bonds. In essence the resonance represents both $\text{Si}(\text{OSi})_4$ at around -110 ppm and $\text{Si}(\text{OSi})_{4-x}(\text{OP})_x$ at more negative values for the chemical shift. Further evidence for Si-O-P bond formation is provided by the ^{31}P resonances at -23 and -30 ppm in the spectrum of 10P-400 which suggest that at this temperature condensation between the siloxane network and the metaphosphate chains or with the branched $[\text{PO}_4]$ tetrahedra occurs. However, the narrow ^{31}P resonance at 0 ppm together with the one at *ca.* -10 ppm still testify to the presence of molecules of ortho- and pyrophosphoric acid in the glassy matrix. On the other hand, after heating the 10P sample to 1000°C a single ^{31}P resonance at *ca.* -37 ppm is seen in the corresponding ^{31}P MAS NMR spectrum, Fig. 3, indicating that the condensation process is complete by 1000°C . Although the observed value for ^{31}P resonance (-37 ppm) is very close to the ones found by Dupree *et al.*⁵ in $\text{Na}_2\text{O-SiO}_2\text{-P}_2\text{O}_5$ glasses and by Nogami *et al.*⁸ in $\text{SrO-SiO}_2\text{-P}_2\text{O}_5$ glasses, the large chemical shift anisotropy clearly shows that the phosphorus must be present as phosphoryl $\text{O}=\text{P}(\text{OP/Si})_3$ rather than $[\text{PO}_4]$. Although the further reduction in the Q_3 resonance intensity to 0.11 and the broadening of the ^{29}Si resonance at -114 ppm in the spectrum of 10P-1000 confirm that the condensation process is largely complete, it does suggest that some amorphous silica network elements must still be present. It is not possible though to distinguish between a structure involving discrete domains of silica matrix and random residual elements of Q_3 units within a phosphosilicate network.

The XRD pattern of 30P-400, Fig. 2(b), shows that crystallization occurs at an early stage yielding a precipitate of very small crystals in the amorphous matrix. At the same time, the heat treatment of 30P at 400°C produces a broadening of the ^{29}Si resonance at -115 ppm together with a loss of intensity in the -211 ppm resonance and an increase in intensity at -215 ppm, Fig. 4. However, as the integrated intensities in Table 3 show there are essentially no changes in the fractions of silicon seen in the different environments. Changes in the ^{31}P NMR spectrum are, in contrast, much more apparent; a significant enhancement in the intensity of the ^{31}P resonance at -42 ppm together with a largely unchanged resonance at 0 ppm. These results suggest that the crystallization process at this stage only involves phosphorus structural units joined with the silicate framework while residual phosphorus precursor remains trapped into the amorphous matrix as molecules of orthophosphoric acid and as a very small amount of pyrophosphoric acid. Heating the 30P gel to 1000°C , while resulting in the growth of a crystalline phase, also leaves an amorphous phase as shown by the broad background in the XRD pattern, Fig. 2(a). The crystalline phase has been previously³ attrib-

uted to $\text{Si}_3(\text{PO}_4)_4$ on the basis of the agreement of the XRD pattern of 30P-1000, Fig. 2(a), with the JCPDS card 22-1380. Nevertheless, these lines also match with those of JCPDS card 40-457, corresponding to $\text{Si}_5\text{O}(\text{PO}_4)_6$, because the structures of the above phases are very similar containing $[\text{PO}_4]$ tetrahedra linking both $[\text{SiO}_6]$ octahedra and $[\text{SiO}_4]$ tetrahedra.^{9,10} The devitrification of gel-derived phosphosilicate glasses has been extensively studied.^{16-20,29} On the one hand the crystallizing phases in the gel-derived phosphosilicate glasses have been assigned to $\text{Si}_5\text{O}(\text{PO}_4)_6$ by XRD and MAS NMR.^{16,17,20,29} On the other hand, XRD and FTIR have been used to identify the crystallizing phases in the gel-derived phosphosilicate glasses as either SiP_2O_7 ¹⁸ or a mixture of $\text{Si}_3(\text{PO}_4)_4$ and SiP_2O_7 phases.¹⁹ Consistent with the XRD the ^{31}P MAS NMR spectrum of 30P-1000 clearly shows the presence of two components, one of which can be assigned to an amorphous material and the other a crystalline one based on their linewidths. Crystalline phases tend to give narrower resonances because their greater order leads to a smaller chemical shift dispersion. Thus the broad resonance with spinning sidebands at -35 ppm can be assigned to an amorphous phosphoryl type material as in the case of the 10P, while the sharp resonance at -44 ppm is assigned to the crystalline material. Obtaining accurate fractions for the two is complicated by the broad nature of the resonance at -35 ppm and its spinning sidebands as well as the overlapping nature of the second component at -44 ppm. A rough estimate based on curve fitting is that the amorphous material represents 56% of the total. The ^{29}Si MAS NMR spectrum of 30P-1000 shows a broad resonance at -115 ppm with a narrow resonance slightly offset from the top at -120 ppm and two narrow resonances at -215 and -218 ppm, Fig. 4. As with the ^{31}P NMR spectrum the narrow resonances can be associated with a crystalline phase while the broad resonance arises from an amorphous material. Such a spectrum is very similar to the one observed for the silicon phosphate glass heat treated for 6 h at 1000°C by Weeding *et al.*⁹ as part of a study of the crystallization behaviour of silicon phosphate glasses at different temperatures. They found that the crystallizing phases were a mixture of $\text{Si}_5\text{O}(\text{PO}_4)_6$ and SiP_2O_7 at low temperature (16 h at 850°C and 6 h at 1000°C) while at high temperature (1300°C) only SiP_2O_7 crystals were found.⁹ By comparing the ^{29}Si MAS NMR spectrum of the devitrified sample containing only SiP_2O_7 with those which contain different relative amounts of both crystalline components, the authors⁹ assigned the ^{29}Si resonances at -120 and -217 ppm to four- and six-coordinated silicon in the $\text{Si}_5\text{O}(\text{PO}_4)_6$ phase. It is worthwhile noting that previous assignments of the phase present to $\text{Si}_5\text{O}(\text{PO}_4)_6$ ^{16,17,20,29} are based on these data.⁹ More recently the ^{29}Si chemical shifts in $\text{Si}_5\text{O}(\text{PO}_4)_6$ have been re-examined and values of -119 ppm for tetrahedral Si together with -213 and -217 ppm have been found.²⁸ The latter two resonances occur in the ratio of 2:1, as predicted from the crystal structure. In addition, the ^{31}P chemical shift was found to be -44 ppm.²⁸ Further evidence supporting the assignment of the observed resonances in 30P-400 to the $\text{Si}_5\text{O}(\text{PO}_4)_6$ phase can be found from the observed chemical shifts for silicon mono- ($\text{Si}_3(\text{PO}_4)_4$) and di- (SiP_2O_7) phosphate.²⁷ Thus silicon monophosphate only exhibits a single narrow ^{31}P resonance at -44.5 ppm consistent with a single crystallographically nonequivalent phosphorus position whereas silicon diphosphate shows a number of resonances in the range -45 to -73.3 ppm arising from different polymorphs. This result together with the lack of reflections in the XRD pattern of 30P-1000, Fig. 2(a), that could be assigned to crystalline SiP_2O_7 , allows us to assign the crystallizing phase to $\text{Si}_5\text{O}(\text{PO}_4)_6$. Therefore the resonances at -120 and -215 , -218 ppm in the ^{29}Si MAS NMR spectrum of 30P-1000 can be related to the four- and six-

coordinated silicons in a crystalline $\text{Si}_5\text{O}(\text{PO}_4)_6$ phase while the resonance observed at -211 ppm at the intermediate temperatures is from six-coordinated silicons in a phase such as $\text{Si}(\text{HPO}_4)_2 \cdot \text{H}_2\text{O}$. The absence of a clear resonance at -120 ppm in the 30P-400 sample can be attributed to the poorly crystalline character of the phase at this temperature; as a result of which, the resonance is broadened sufficiently to be included in the -115 ppm resonance lineshape. This interpretation is supported by the marked sharpening of the other resonances attributed to the crystalline phase, -215 and -218 ppm between 400°C and 1000°C . Despite the close similarity between the actual 30P P:Si molar ratio of 1:1.28 and that of 1:1.2 required for the $\text{Si}_5\text{O}(\text{PO}_4)_6$ phase, crystallisation of this phase is incomplete after the heating cycle employed. This is a consequence of the high connectivity of the amorphous framework and the absence of modifier cations making the crystallization process more difficult.

An explanation for the differing behaviour of the two gel compositions can be found in the local Si:P ratio of the gel. In both the 10P and 30P gels phosphorus is distributed non-uniformly, tending to be concentrated within the pore structure of the siloxane framework. In the case of the 10P gel the low concentration of the Q'_N units means that although the local gel composition may lie within the required Si:P ratio of $\sim 1:1$, this will only be true for a very small domain which cannot act as a nucleus for subsequent crystallisation and consequently the 10P gel keeps its amorphous nature up to 1000°C and shows no clear evidence of six-coordinated silicon. However, for the 30P gel, the greater amount of P_2O_5 in the gel composition means that the required Si:P ratio is attained over a larger domain allowing the formation of microcrystallites of a phase containing Si–O–P bonds.

5. Conclusion

Solid state ^{29}Si and ^{31}P MAS NMR have been used to investigate the microstructural changes that occurred in 10P and 30P gels during their conversion from a gel to the corresponding gel-derived glasses by heating. It was found that both dried gels (100°C) have very similar structures formed by a siloxane framework containing silanol groups and including isolated molecules of orthophosphoric acid and a very small amount of pyrophosphoric acid. In spite of this, heating the studied gels to 300°C caused different structural rearrangements of their glassy matrix. For the 10P gel P–O–Si bonds are not formed at this stage; only a partial dehydroxylation occurs between silanol groups increasing the degree of polymerisation of the siloxane network. In marked contrast, P–O–Si bonds were formed after heating the 30P gel to the same temperature. The differing behaviour of the studied gels on heating mirrors a difference in the distribution of phosphorus atoms on the atomic scale in the pores of the siloxane framework. Local concentration inhomogeneities are greater for the gels with higher phosphorus compositions thus permitting the attainment of the required Si:P ratio over large enough regions to act as nucleation sites for a crystalline phosphosilicate.

Acknowledgements

The work was supported on behalf of the National Research Council of Italy (CNR), Targeted Project ‘‘Special Materials for Advanced Technologies II’’ (No. 980014 PF34).

References

- 1 M. Nogami, K. Miyamura and Y. Abe, *J. Electrochem. Soc.*, 1997, **144**, 2175.
- 2 M. Nogami, C. Wang and Y. Abe, *Fast proton conducting P_2O_5 – SiO_2 glasses*, in *Proc. XVIII Cong. On Glass*, Am. Ceram. Soc., San Francisco, USA, vol. D3, 1998, pp. 139–144.
- 3 M. D’Apuzzo, A. Aronne, S. Esposito and P. Pernice, *J. Sol–Gel Sci. Technol.*, 2000, **17**, 247.
- 4 L. L. Hench, *J. Am. Ceram. Soc.*, 1991, **74**, 1487.
- 5 R. Dupree, D. Holland and M. G. Mortuza, *Nature*, 1987, **328**, 416.
- 6 R. Dupree, D. Holland, M. G. Mortuza, J. A. Collins and M. W. G. Lockyer, *J. Non-Cryst. Solids*, 1989, **112**, 111.
- 7 M. W. G. Lockyer, D. Holland and R. Dupree, *Phys. Chem. Glasses*, 1995, **36**, 22.
- 8 M. Nogami, K. Miyamura, Y. Kawasaki and Y. Abe, *J. Non-Cryst. Solids*, 1997, **211**, 208.
- 9 T. L. Weeding, B. H. W. S. de Jong, W. S. Veeman and B. G. Aitken, *Nature*, 1985, **318**, 352.
- 10 H. Makart, *Helv. Chim. Acta*, 1967, **50**, 399.
- 11 E. Tillmanns, W. Gebert and W. H. Baur, *J. Solid State Chem.*, 1973, **7**, 69.
- 12 C. J. Brinker, A. J. Hurd, P. R. Schunk, G. C. Frye and C. S. Ashley, *J. Non-Cryst. Solids*, 1992, **147&148**, 424.
- 13 B. E. Yoldas, *J. Sol–Gel Sci. Technol.*, 1993, **1**, 65.
- 14 J. Livage, P. Barboux, M. T. Vandendorre, C. Schmutz and F. Taulelle, *J. Non-Cryst. Solids*, 1992, **147&148**, 18.
- 15 F. Tian, L. Pan and X. Wu, *J. Non-Cryst. Solids*, 1988, **104**, 129.
- 16 S.-P. Szu, L. C. Klein and M. Greenblatt, *J. Non-Cryst. Solids*, 1992, **143**, 21.
- 17 C. Fernandez-Lorenzo, L. Esquivias, P. Barboux, J. Maquet and F. Taulelle, *J. Non-Cryst. Solids*, 1994, **176**, 189.
- 18 M. Laczka and M. Ciecinska, *J. Sol–Gel Sci. Technol.*, 1994, **3**, 219.
- 19 Y. S. Kim and R. E. Tressler, *J. Mater. Sci.*, 1994, **29**, 2531.
- 20 Z. Cao, B. I. Lee, W. D. Samuels, L. Q. Wang and G. J. Exarhos, *J. Mater. Res.*, 1998, **13**, 1553.
- 21 I. A. Voinovitch, J. Debras-Guedon and J. Louvrier, *L’analyse des silicates*, Hermann, Paris, 1962, p. 467.
- 22 H. Bennet and W. G. Hawley, *Methods of silicate analysis*, Academic Press, London, 1965, p. 130.
- 23 C. M. Schramm, B. H. W. S. de Jong and V. E. Parziale, *J. Am. Chem. Soc.*, 1984, **106**, 4396.
- 24 A. R. Grimmer, M. Magi, M. Hahnert, H. Stade, A. Samoson, W. Wieker and E. Lippmaa, *Phys. Chem. Glasses*, 1984, **25**, 105.
- 25 R. K. Brow, R. J. Kirkpatrick and G. L. Turner, *J. Non-Cryst. Solids*, 1990, **116**, 39.
- 26 P. Hartmann, J. Vogel and B. Schnabel, *J. Non-Cryst. Solids*, 1994, **176**, 157.
- 27 P. Hartmann, C. Jana, J. Vogel and C. Jager, *Chem. Phys. Lett.*, 1996, **258**, 107.
- 28 T. R. Krawietz, P. Lin, K. E. Lotterhos, P. D. Torres, D. H. Barich, A. Clearfield and J. F. Haw, *J. Am. Chem. Soc.*, 1998, **120**, 8502.
- 29 L. Q. Wang, W. D. Samuels, G. J. Exarhos, B. I. Lee and Z. Cao, *J. Mater. Chem.*, 1998, **8**, 165.